

# Investigation of water diffusion mechanisms in relation to polymer relaxations in polyamides

Florentina-Maria Preda,<sup>†</sup> Angel Alegría,<sup>‡</sup> Anthony Bocahut,<sup>¶</sup> Louise-Anne Fillot,<sup>†</sup> Didier R. Long,<sup>†</sup> and Paul Sotta<sup>\*,†</sup>

*Laboratoire Polymères et Matériaux Avancés, CNRS/Solvay, UMR5268, Axel'One, 87 avenue des Frères Perret, 69192 Saint Fons Cedex, France, Centro de Fisica de Materiales, P. Manuel de Lardizabal 5, E-20018 San Sebastian, Spain, and Advanced Polymers and Materials Department, Solvay, UMR5268, Axel'One, 87 avenue des Frères Perret, 69192 Saint Fons Cedex, France*

E-mail: paul.sotta-exterieur@solvay.com

July 27, 2015

## Abstract

Diffusion in semi-crystalline polymers is a complex phenomenon because of the existence of specific interactions (non-polar or polar), dynamic heterogeneities and crystalline phases. The diffusion of water in two semi-crystalline polyamide (PA6,6 and PA6,10) was investigated in order to determine the diffusion mechanisms and the influence of polymer relaxations on this process. Liquid water diffusion follows a Fickian mechanism in PA6,10 and a non-Fickian or anomalous mechanism in PA6,6.

---

\*To whom correspondence should be addressed

<sup>†</sup>Laboratoire Polymères et Matériaux Avancés, CNRS/Solvay, UMR5268, Axel'One, 87 avenue des Frères Perret, 69192 Saint Fons Cedex, France

<sup>‡</sup>Centro de Fisica de Materiales, P. Manuel de Lardizabal 5, E-20018 San Sebastian, Spain

<sup>¶</sup>Advanced Polymers and Materials Department, Solvay, UMR5268, Axel'One, 87 avenue des Frères Perret, 69192 Saint Fons Cedex, France

Through a quasi-equilibrium experiment in Dynamic Vapor Sorption, it is shown that this difference results from the dependence of the diffusion coefficients on water concentration. Moreover, the influence of the polymer relaxations was assessed by Broadband Dielectric Spectroscopy. The dielectric characteristic relaxation times of the  $\alpha$  relaxation, associated to the glass transition, and of the  $\beta$  relaxation, related to more local dynamics, have been measured. A simple comparison with the timescale of diffusion suggests that diffusion and polyamide  $\alpha$  relaxation should not be directly correlated. However, diffusion is correlated to the secondary  $\beta$  relaxation, **which encompasses the local chain dynamics of hydrogen bonded amide groups in the presence of water.** A mechanism of diffusion based on the trapping of water molecules between neighboring sorption sites (amide groups) is proposed in these strongly interacting polymers. It is suggested that diffusion is limited by the relaxation time of hydrogen bonds between water molecules and amide groups and the change in conformation of these amide groups present in polyamides.

## 1 Introduction

Polyamides are a family of semi-crystalline thermoplastic polymers widely employed in the automotive industry due to its excellent thermal stability and mechanical properties. However, polyamide can be significantly affected by the absorption of low molecular weight penetrants<sup>1</sup> like water from the air humidity or ethanol in biofuels. Water sorption is accompanied by a large decrease in the glass transition temperature,<sup>2,3</sup> which strongly affects mechanical properties.<sup>1</sup> The rate of sorption and amount of absorbed water depend on the mechanisms of interaction between water and polyamide, along with sorption and diffusion mechanisms. Therefore, these aspects have been intensively studied in the literature.<sup>2-13</sup> It is generally accepted that water interacts with amide groups to replace the initial hydrogen bonds between them.<sup>4,6,10,14</sup> It has been proposed that several water populations exist (tightly and loosely bound water) and that water molecules organize in clusters beyond a

certain solvent uptake.<sup>5,7</sup>

Diffusion and sorption of solvents in polymers can be very complex because of the existence of specific interactions (non-polar or polar), dynamic heterogeneities in the amorphous phase, **modification of the polymer dynamics induced by the solvents** and different crystalline phases. In polyamide/water systems, all of these factors have to be taken into account. To begin with, water interacts strongly with amide groups and leads to the decrease of the glass transition temperature, or plasticization of the amorphous phase, i.e. an increase in the mobility of the polymer chains.<sup>15</sup> Secondly, although the crystalline phase is considered impermeable to the solvent,<sup>16,17</sup> its existence induces a gradient of mobility in the amorphous phase, which has often been depicted as a Rigid Amorphous Fraction.<sup>18</sup> **As a consequence, the whole amorphous phase may not be equally accessible to solvents. Indeed, a large number of studies have been dedicated to elucidating the accessibility of the amorphous phase. While it was estimated that roughly one third of the amorphous phase is in the interlamellar space and two thirds outside the lamellar stacks<sup>19</sup>, water was found to diffuse in all amorphous regions.<sup>16</sup> Water molecules in the interlamellar regions are thought to be tightly bounded.<sup>20</sup>**

**Differences in the mobility of the amorphous phase have been studied by NMR.<sup>21-23</sup> It was found that water diffuses preferentially in the soft amorphous phase, which is then plasticized by the water molecules.**

Previous literature studies have been focused on sorption or diffusion experiments of water in dry polyamide at a certain activity. The diffusion mechanisms are either Fickian<sup>3</sup> or non-Fickian,<sup>11</sup> depending on the polymer characteristics and on processing conditions. In one of the most complete studies on water diffusion in polyamide, Lim et al<sup>2</sup> have determined that diffusion coefficients increase as a function of water activity and temperature. Each measurement was done with a dry polyamide as a starting material, which means that water diffuses in a polymer matrix gradually plasticized, subject to swelling and probably with a gradient in water concentration.

**Spatially resolved water uptake was studied quantitatively by NMR imaging.<sup>24-28</sup> Recent**

studies have also shown that a plasticization lag exists, meaning that a few percentages of water were absorbed in the material before plasticization was visible.<sup>28</sup>

Thus, it would be interesting to study if there is a correlation between penetrant diffusion and the mobility of the polymer chains due to amorphous phase heterogeneity or plasticization. To our knowledge, no previous study has investigated the correlation between the diffusion coefficient and the polymer relaxations (main  $\alpha$  relaxation and more local, secondary relaxations) in polyamides.

In order to decouple polymer relaxations and water diffusion, we have adopted a step-by-step experiment by using Dynamic Vapor Sorption (DVS). In DVS experiments, a polymer film can be kept through small activity steps from 0.1 to 0.9 so that the polymer reaches equilibrium at each step at water activity  $a$  before the next sorption experiment is launched at activity  $a + \Delta a$ . Therefore, the system should stay close to thermodynamic equilibrium when a new water population diffuses. If the activity steps are sufficiently small, diffusion occurs in a homogeneously relaxing environment, with limited swelling and a relatively constant water concentration. In this way, we might thus isolate diffusion and polymer relaxations from other phenomena and test the correlation between these two processes.

The objective of this study is to investigate the relationship between water diffusion and the various relaxation processes in polyamides. For this, we have measured water diffusion coefficients and the polymer relaxation times as a function of water activity. Two different polyamides with slightly different ratios of amide/methylene groups (PA6,6 and PA6,10), obtained with different processing conditions, have been studied. The main purpose is to understand diffusion mechanisms, in particular whether or not diffusion is coupled to polymer relaxation. The influence of the ratio of amide/methylene groups, i.e. the density of hydrogen bonds, is tentatively discussed.

## 2 Materials and methods

### 2.1 Materials

PA6,6 and PA6,10 pellets were provided by Solvay and contained no stabilizers or fillers. PA6,6 films 100  $\mu\text{m}$  thick were obtained by film-cast extrusion. PA6,10 plates  $0.8 \times 100 \times 100$  mm were obtained by injection-molding with a DEMAG H200-80T press. The plates were thinned at 300  $\mu\text{m}$  using a planer.

Prior to all experiments, the films were dried for 24h at 110°C for PA6,6 and 80°C for PA6,10. The films were introduced in thermo-sealed envelopes and kept in a desiccator to avoid any contact with air moisture. The characteristics of each film, measured after drying, are: PA6,6 100  $\mu\text{m}$ : glass transition temperature  $T_g = 64 \pm 2^\circ\text{C}$ , melting point  $T_m = 261 \pm 2^\circ\text{C}$ , crystallinity ratio  $\chi_c = 38 \%$ , number average molecular weight  $M_n = 25000$  g/mol and polydispersity  $PI \simeq 2$  (SEC, absolute value, method of N-trifluoroacetylation<sup>29</sup>); PA6,10 300  $\mu\text{m}$ : glass transition temperature  $T_g = 53 \pm 2^\circ\text{C}$ , melting point  $T_m = 222 \pm 2^\circ\text{C}$ , crystallinity ratio  $\chi_c = 23 \%$ , number average molecular weight  $M_n = 37000$  g/mol and polydispersity  $PI \simeq 2$  (SEC, absolute value, method of N-trifluoroacetylation<sup>29</sup>).

### 2.2 Sorption experiments

Polymer films were immersed in liquid water and removed regularly for weighing following a standard procedure: removal from sorption cell, pressing between absorbent paper, surface drying with compressed air, record of weight exactly at 1 minute after removal from sorption cell, re-immersion. The mass intake is recorded as a function of immersion time. Measurements were done at the following temperatures: 25, 40 and 55°C.

For film conditioning at activity 0.5, the films was kept in a humidity-conditioned laboratory. For film conditioning at activities 0.75 and 0.84, saturated salt solutions (NaCl, KCl) were used at room temperature (20°C). The humidity in the atmosphere above a saturated salt solution is tabulated in the literature<sup>30</sup> as a function of temperature. The saturated

salt solution was placed at the bottom of a desiccator. The polymer film was left several days above the saturated salt solution in the closed desiccator until sorption equilibrium was reached. The conditioned films were used for Differential Scanning Calorimetry and Broadband Dielectric Spectroscopy measurements.

No change in the crystalline fraction was observed by DSC after sorption experiments. The crystalline structure was checked by X ray diffracton in the reference and water saturated samples ( $a = 0.3, 0.7$  and  $1$ ). Both polyamides have an  $\alpha$  crystalline lattice. In water saturated samples, Bragg peaks characteristic of the  $\alpha$  crystalline lattice are better resolved, with an increased angular spacing of the two main peaks (100) and (010)/(110), which indicates a change towards a more perfect crystalline phase in the presence of water. This evolution of the crystalline structure during long time sorption experiments has already been reported<sup>16,31</sup>. In order to check the possible impact of this evolution on diffusion and equilibrium sorption, liquid water-saturated films were dried and then re-immersed in liquid water. The new curves of mass uptake superimpose perfectly to the initial ones up to equilibrium values, meaning that the crystalline transformation does not impact diffusion kinetics or equilibrium sorption.

### 2.3 Dynamic Vapor Sorption (DVS)

A DVS Advantage device was used for the sorption of water vapor at controlled activity ( $a = P/P_{sat}$ ). The DVS Advantage Analyzer regulates the pressure inside the sample chamber and an internal microbalance measures the mass uptake of the polymer film. Before sorption at temperature  $T$ , the dried films were exposed to a dry nitrogen flow at  $T$  until their weight was stable. Activity steps of 0.1 were then applied in the range of 0.1 to 0.9. Each activity was maintained for 2 days to ensure that the sorption equilibrium was reached. After 2 days at activity  $a$ , the device sets the next activity  $a+0.1$  almost instantaneously (equilibration time of new activity is shorter than 1 minute)and a new mass intake is recorded. Measurements were done at 29, 35, 40 and 51°C for PA6,6 and 29, 40 and 51°C for PA6,10. For the two

polymers, measurements at 51°C stopped at activity 0.4 for PA6,6 and activity 0.6 for PA6,10 because the experimental temperature was too close to the limit of the machine (60°C).

## 2.4 Differential Scanning Calorimetry (DSC)

A TA Instruments DSC Q2000 was used in the standard mode (ramp 10°C/min) to determine the melting point and the crystalline ratio and in the modulated mode (MDSC) to determine the glass transition temperature  $T_g$  of pristine and water equilibrated polymer. MDSC was essential to this study because the glass transition of polyamide films could not be clearly determined in standard mode, as is sometimes the case in polyamides. A Liquid Nitrogen Cooling System (LNCS) was used with a Helium flow (25 ml/min) to have access to very low temperatures (down to  $-180^\circ\text{C}$ ). Samples (between 7 and 15 mg) were placed in non-hermetic aluminium pans and heated between  $-150$  and  $150^\circ\text{C}$  at a heating rate of  $3^\circ\text{C}/\text{min}$  with a temperature modulation of  $\pm 2^\circ\text{C}$  every 60 s. The water-swollen samples were transferred rapidly between the sorption cell and the DSC pans in order to limit solvent evaporation. The glass transition temperature was determined as the mid-height or inflexion point in the reversible heat flow.

## 2.5 Dielectric Spectroscopy

Three main relaxation processes due to rotational fluctuations of the molecular dipoles have been identified in polyamides.<sup>32</sup> A highest frequency, the  $\gamma$  relaxation is generally attributed to very fast rotation of the aliphatic sequences. These very local motions are internal to the monomer. The  $\beta$  relaxation is generally attributed to the motion of the amide group dipoles, while the  $\alpha$  relaxation is related to larger scale motions associated to the glass transition. Motions involved in the  $\beta$  and  $\alpha$  relaxations may potentially be coupled to or influenced by the motions of water molecules.<sup>13,33–35</sup> We thus focus here on these processes. The corresponding relaxation times have been measured by dielectric spectroscopy as a function of temperature and at various water activities.

In dielectric spectroscopy, relaxation processes can be identified through the variations of the frequency dependent complex permittivity  $\epsilon_{dielec}^*(\omega)$ , or equivalently complex modulus  $M_{dielec}^*(\omega)$  or complex conductivity  $\sigma^*(\omega)$ . In addition to dipole reorientations, charge transport and interfacial polarization effects take place. The  $\alpha$  relaxation time  $\tau_\alpha$  is **often difficult to measure in polyamides** because it is accompanied by a strong increase of the sample conductivity. **Other phenomena (electrode polarization, Maxwell-Wagner-Sillars polarization<sup>36</sup>) can also have a contribution (visible above the  $\alpha$  peak on the high temperature side in Figure 1).**  $\tau_\alpha$  was determined by using the maximum of the loss permittivity and/or the loss modulus in isochronal curves (Figure 1). Although this method may seem less precise than fitting the relaxation curves in isothermal representation, it was preferred because it provides relaxation times over a larger temperature range. When both isochronal and isothermal representations could be used, it was checked that the data coincide. The loss modulus representation is less sensitive to contributions from sample conductivity and gives a well-defined peak. The values obtained from the loss modulus are shifted with respect to the values obtained from the loss permittivity but allow a verification of the latter. A typical curve of obtained  $\tau_\alpha$  is shown in Figure 2. As it can be seen, the two curves are roughly parallel but shifted in frequency.

The variation of the  $\alpha$  relaxation times in polymers generally follows a Vogel-Fulcher-Tammann (VFT)<sup>37-39</sup> temperature dependence (equation (1)):

$$\tau(T) = \tau_0 \exp\left(\frac{A_{VFT}}{T - T_0}\right) \quad (1)$$

where  $\tau$  is the relaxation time,  $\tau_0$  the relaxation time in the high temperature limit,  $A_{VFT}$  is a constant and  $T_0$  denotes the Vogel temperature, generally found to be 30 – 70 K below the glass transition temperature  $T_g$ .<sup>36</sup>

The  $\beta$  relaxation is strongly affected by the presence of water.<sup>13</sup> In a dry polyamide, the  $\beta$  relaxation is symmetrical **and corresponds to the relaxation denoted  $\beta_{dry}$  in Figure**



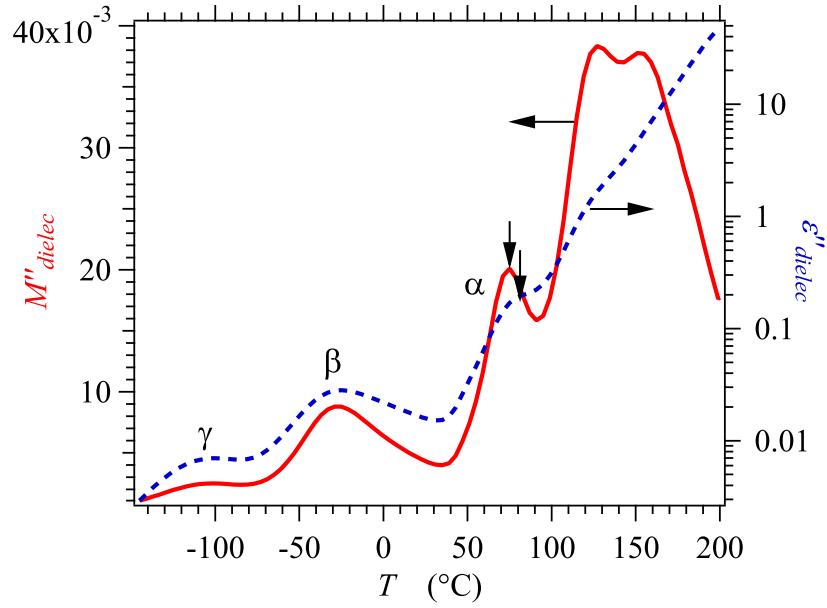


Figure 1: Isochronal representation of loss permittivity (dotted curve) and loss modulus (full curve) as a function of temperature for dry PA6,6 at the frequency of 133 Hz. The maximum of the  $\alpha$  relaxation peak is pointed by arrows.

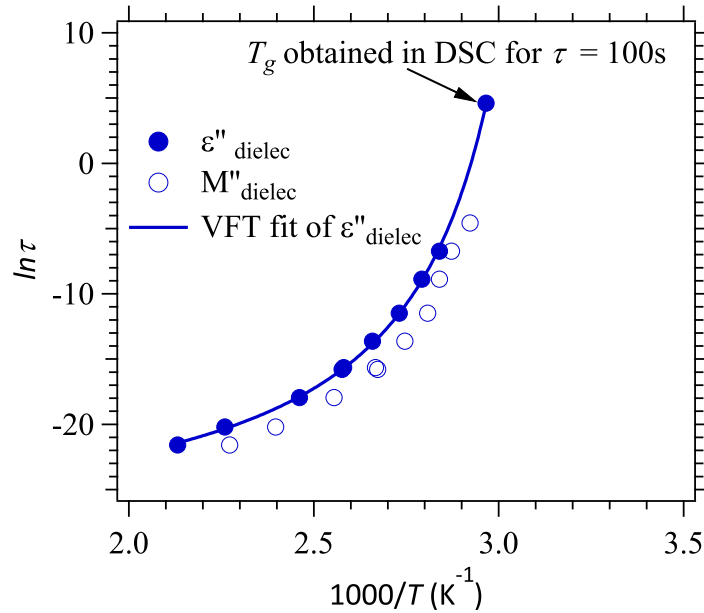


Figure 2: Relaxation times as a function of temperature obtained from  $\epsilon''_{dielec}$  and  $M''_{dielec}$  isochronal representation for dry PA6,6. Solid line represents a Vogel-Fulcher-Tammann fit of the data.

3. When water is introduced, the initial position of the beta relaxation does not change significantly but a second, more intense beta relaxation (denoted  $\beta_w$  in Figure 3) appears in the high frequency side. As the water concentration increases, this relaxation shifts to higher and higher frequencies. It should be highlighted that in PA6,10, two relatively well distinct processes can be observed in the presence of water (Figure 3 (a)). In PA6,6 however, it is very difficult to clearly distinguish between the two processes, especially at high water activities (Figure 3 (b)). For this reason, the position of the  $\beta$  relaxation determined for the dry polymer was introduced manually in the fits, with varying dielectric strength. The relaxation denoted  $\beta_w$  is considered to be representative of the local chain dynamics of hydrogen bonded amide groups in the presence of water. It is thus the one discussed in this work in relation to water diffusion.

It should be highlighted that polymer processing and the resulting distribution of rigid and mobile amorphous fractions can have an influence on polymer relaxations. A comparison has been done between the PA6,6 100  $\mu\text{m}$  film and a PA6,6 0.8 mm injected plate. The effect of processing is mainly noticeable on the  $\alpha$  relaxation associated to the glass transition, since the crystalline fractions and the glass transition temperatures of the two samples are slightly different. However, no effect was noticed on the secondary, more local  $\beta$  or  $\gamma$  relaxations, for which the obtained characteristic relaxation times superimposed. As a consequence, the characteristic relaxation times presented in this paper can be extended to polyamides prepared with different processing methods.

A Novocontrol Alpha Analyzer and a Quatro temperature control system were used to conduct experiments under a voltage of 3V in the temperature range of  $-130$  to  $200^\circ\text{C}$  with  $4^\circ\text{C}$  steps. For each temperature, the frequency range was  $10^{-2}$  Hz to  $10^6$  Hz (Broadband Dielectric Spectroscopy - BDS). For dry samples, additional experimental points in the frequency range  $10^6$  Hz to  $10^9$  Hz were obtained by High Frequency Dielectric Spectroscopy (HFDS) under a voltage of 0.5 V in the temperature range  $-130$  to  $200^\circ\text{C}$  with  $1^\circ\text{C}$  steps. Polymer films were cut into disks of 30 mm (BDS) and 10 mm (HFDS) di-

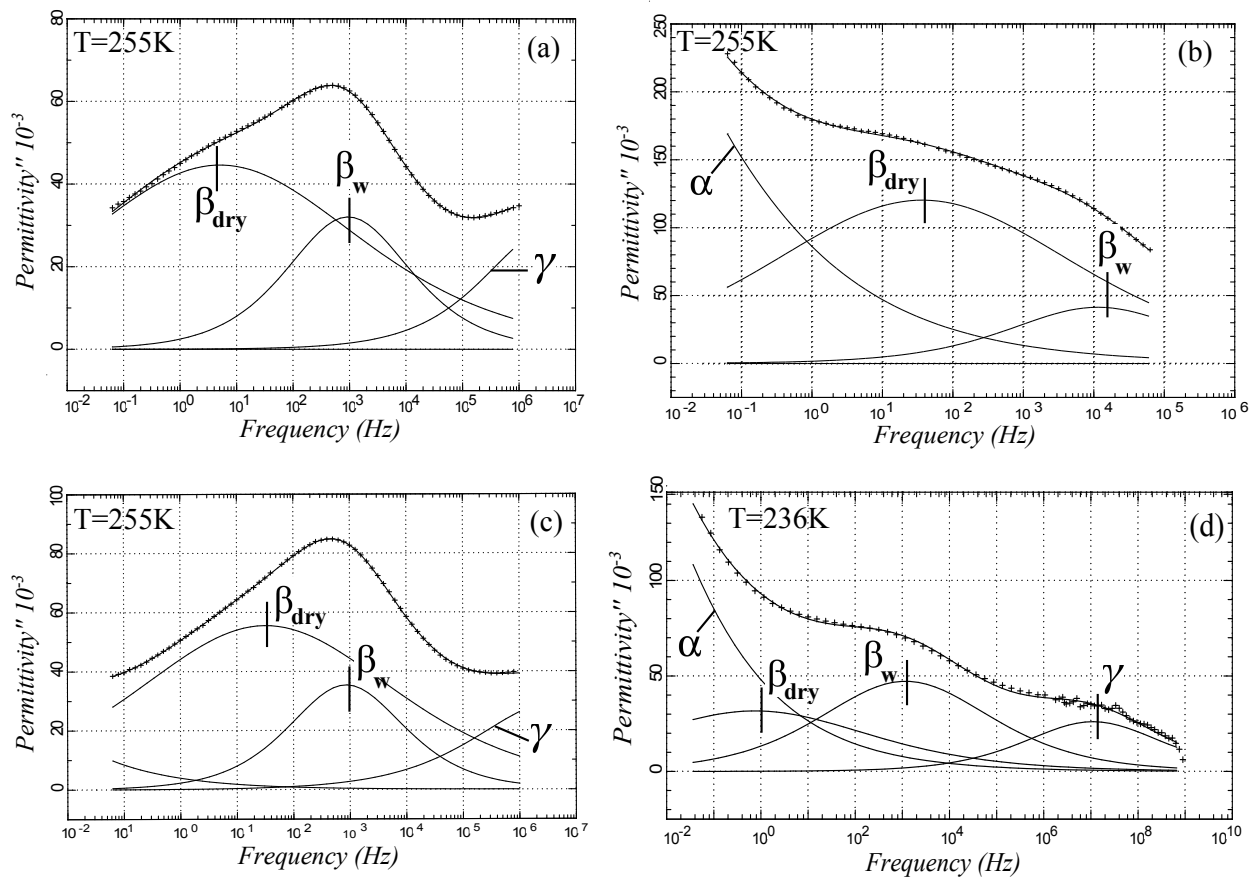


Figure 3: Isotherms of loss permittivity  $\epsilon''$  in the region of the  $\beta$  relaxation in (a) PA6,10 at water activity 0.11 (left) and 1 (right) and (b) PA6,6 at water activity 0.11 (left) and 1 (right), together with corresponding Havriliak-Negami fits.

ameter and placed between gold plated electrodes. For water-equilibrated samples, the electrode/polymer film/electrode sandwich was immediately quenched at  $-130^{\circ}\text{C}$  to avoid solvent evaporation. Measurements were performed on heating. Polymer films kept a constant weight up to  $25 - 35^{\circ}\text{C}$ , depending on the initial water concentration. Above this temperature, water evaporation started to occur as was illustrated by the decrease in the real part of permittivity  $\epsilon'$  for all frequencies around  $100^{\circ}\text{C}$ .

## 2.6 Analysis of sorption curves

Based on the impact of the penetrant on the polymer matrix, different types of diffusion may occur<sup>40</sup>:

- *Case I or Fickian*: diffusion occurs in a polymer matrix which is unperturbed by the presence of solvent and the diffusion coefficient of the solvent is independent of the solvent concentration, within the duration of the sorption experiment.
- *Case II*: the diffusion coefficient of the solvent depends on the solvent concentration because the polymer matrix is affected (plasticized) by the presence of solvent. The polymer relaxation rate becomes faster than the diffusion rate. Consequently, the penetrant moves into a polymer with a steep concentration front separating regions of swollen, penetrant saturated polymer behind the front and unswollen, dry polymer ahead of the front.
- *Anomalous or non-Fickian diffusion*:<sup>41</sup> polymer relaxation rates and diffusion rates are similar. As in Case II diffusion, the penetrant induces swelling in the polymer matrix but the phenomenon is delayed. Therefore, a slowly advancing front of swelling is preceded by a Fickian diffusion tail.

In order to properly interpret sorption curves, it is therefore essential to (1) check the variation of the diffusion coefficient along the sorption process and (2) relate diffusion time

scale to the characteristic relaxation time related to the various relaxation processes displayed by the polymer chains.

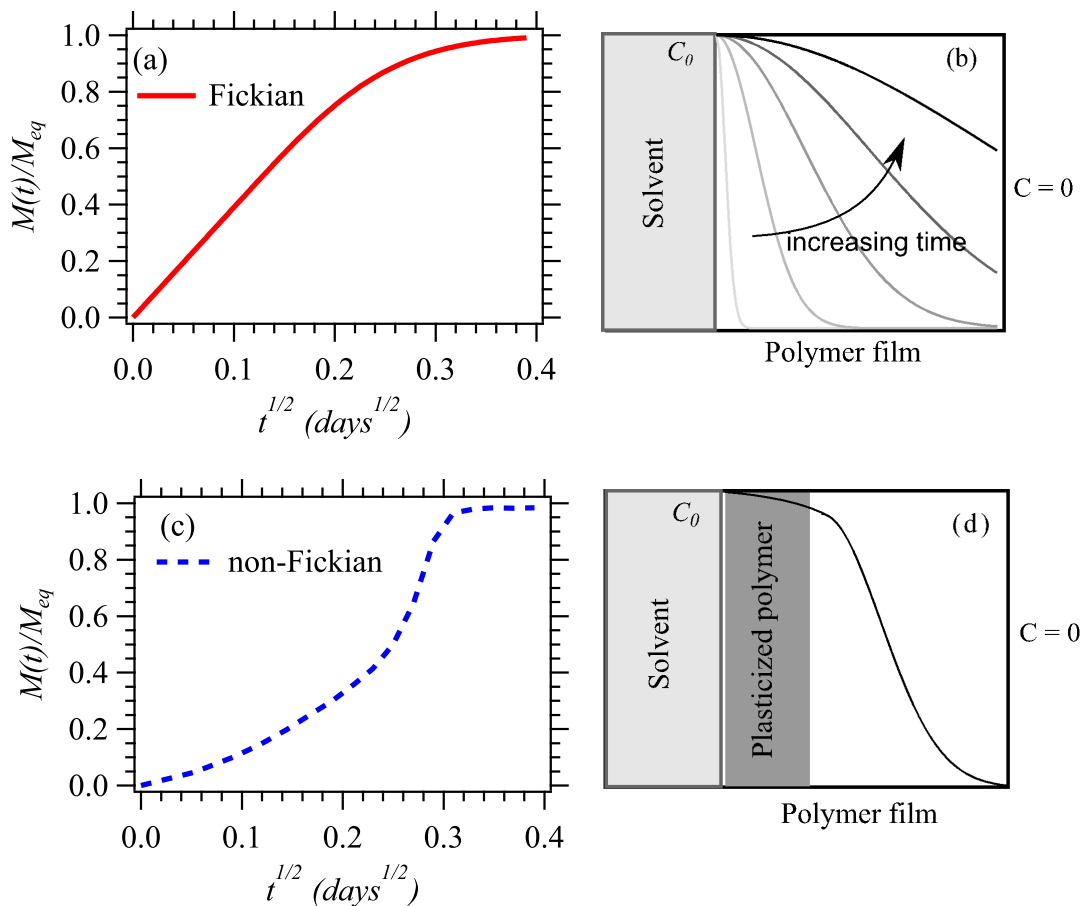


Figure 4: Schematic representation of sorption curves following (a)Fickian and (c)non-Fickian diffusion mechanisms and (b),(d) their corresponding solvent concentration profiles

The sorption data acquired for the polymer-solvent system is generally represented as the normalized mass intake  $M(t)/M_{eq}$ , which is the ratio between the mass uptakes at time  $t$  and at equilibrium. We consider the case of one-dimensional diffusion in a polymer film so thin that all the penetrant enters through the plane faces and a negligible amount through the edges. The film of thickness  $l$  is suspended in a sorption cell where the solvent activity or partial pressure remains constant. In this geometry, Fickian diffusion (with a constant diffusion coefficient  $D$ ) is described by an exact mathematical model, which gives

the following equation:<sup>42</sup>

$$\frac{M(t)}{M_\infty} = 1 - \sum_{n=0}^{\infty} \frac{8}{(2n+1)^2\pi^2} \exp\left(\frac{-D(2n+1)^2\pi^2 t}{l^2}\right) \quad (2)$$

At short times, Equation 2 gives a linear increase of the normalized mass intake  $M(t)/M_{eq}$  as a function of  $t^{1/2}$  and the diffusion coefficient  $D$  is simply extracted from the slope of this curve. Thus, the shape of the  $M(t)/M_{eq}$  curve as a function of  $t^{1/2}$  gives a first information on the diffusion mechanism (Figure 4). In the case of Fickian diffusion, a linear increase with the square root of time is observed for the normalized mass intake, whereas in a non-Fickian mechanism the curve is generally a sigmoid exhibiting an inflexion point. Our curve fits have been strictly limited to the simple case of Fickian diffusion, where diffusion coefficients can be calculated accurately with equation (2).

Several mathematical models have been suggested to analyze non-Fickian diffusion. Berens and Hopfenberg<sup>43</sup> proposed a heuristic model based on the linear superposition of Fickian diffusion and relaxation processes. A more complete model was proposed by Hedenqvist and Gedde,<sup>44</sup> who took into consideration the solute-concentration dependence of diffusivity, swelling, time-dependent surface boundary concentration and swelling-induced mechanical stresses. However, all these models have a large number of adjustable parameters so their physical relevance can be argued. To check the relevance of either model, it is crucial to be able to relate time scales associated to diffusion to the relaxation time of the polymer matrix.

## 3 Results

### 3.1 Sorption kinetics

The sorption of liquid water in the two polyamides was measured at three temperatures (25, 40 and 55°C) (Figure 5). In PA6,10, the normalized water intake  $M(t)/M_\infty$  increases

linearly with  $t^{1/2}$  and a Fickian model fits the experimental data perfectly for all temperatures. The calculated diffusion coefficients are  $3 \times 10^{-9}$ ,  $1.1 \times 10^{-8}$  and  $3.5 \times 10^{-8}$   $\text{cm}^2/\text{s}$  for the three temperatures respectively. Assuming that the diffusion coefficient dependence on temperature follows an Arrhenius law, an activation energy of 66 kJ/mol is obtained for the diffusion of water in PA6,10. This value is within the range of 60 to 80 kJ/mol activation energies reported for diffusion of water in PA6,6.<sup>2,45</sup>

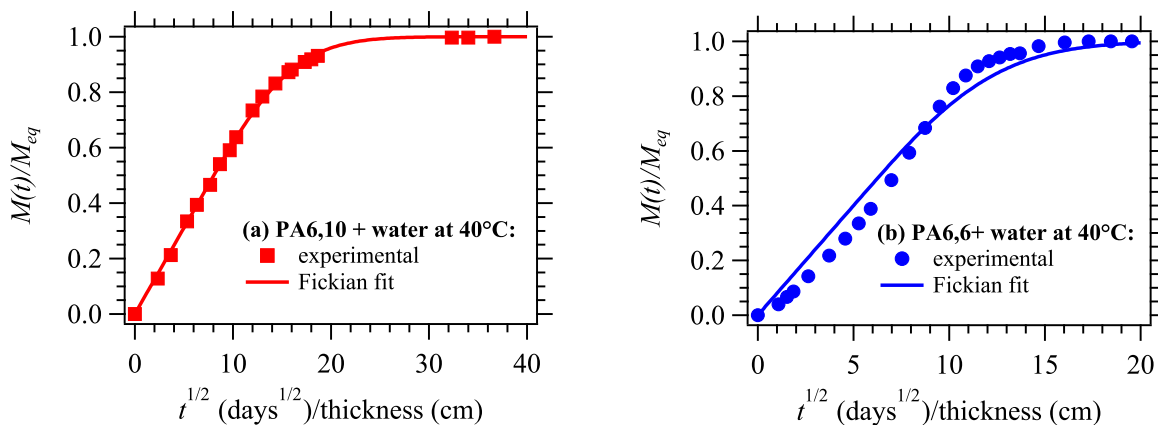


Figure 5: Sorption kinetics of liquid water at 40°C in (a)PA6,10 and (b)PA6,6

The curve obtained for the diffusion of water in PA6,6 at 40°C has a sigmoidal shape with an inflexion point. This indicates that the diffusion mechanism is not Fickian. Consequently, the experimental data cannot be fitted with equation (2). Therefore, other phenomena might occur after a first step of linear Fickian diffusion: concentration dependent diffusion coefficient, swelling and/or polymer relaxation.

A Dynamic Vapor Sorption experiment was designed to separate the diffusion process from other phenomena. Swelling kinetics, polymer relaxation and concentration fronts appear when the solvent/polymer system is not at equilibrium. Intermediate equilibrium states can be obtained by absorbing water at increasing activities. A small upward step of activity results in a small increase of the water content with respect to equilibrium, which should not modify significantly the state of the matrix. Water diffusion should then follow a Fickian mechanism at each activity step. However, for practical reasons related to the precision of

the balance and the time span of the experiment, infinitesimal activity steps cannot be set up. A good compromise consists in increasing the activity by 0.1 in the range 0.1 to 0.9, which cumulates to a maximum span of 3 weeks for an experiment at the lowest temperature. A typical curve obtained following this protocol is shown in Figure 6(a).

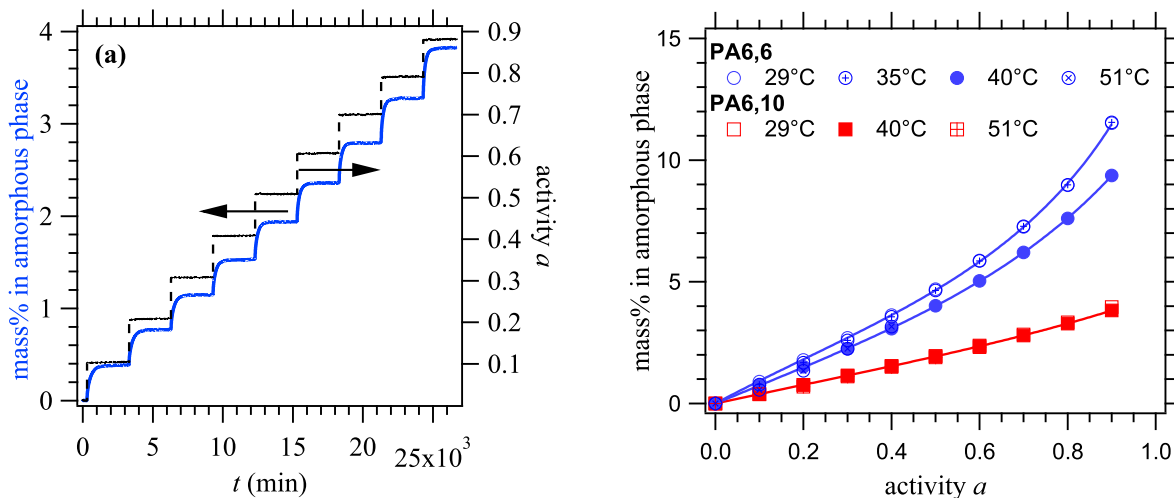


Figure 6: (a) Typical curve obtained in DVS experiments for mass uptake as a function of time; here, water sorption in PA6,10 at 40°C; (b) Sorption isotherms for water in PA6,6 and PA6,10 at different temperatures (for PA6,10, data at all temperatures roughly superimpose; for PA6,6, data at 29 and 35C and data at 40 and 51C roughly superimpose). The full lines were obtained by fitting the data with a GAB model.

The values of water uptake at equilibrium for each activity and temperature are reported in Figure 6(b) as sorption isotherms. **It should be highlighted that sorption isotherms report values at equilibrium and are therefore independent of the DVS protocol.** It is observed that water is more absorbed by PA6,6 than by PA6,10, which is expected since the number of polar amide groups/g of polymer is 25% higher in PA6,6 than in PA6,10, making PA6,6 more hydrophilic. However, the difference in water intake is much higher than the difference in amide group density.

### 3.2 Diffusion coefficients

In order to obtain information on diffusion coefficients, the water uptake for each activity step (see Figure 6(a)) is treated individually and plotted as the normalized mass intake as



a function of the square root of time. Figures 7(a) and (b) illustrate the sorption kinetics of water in PA6,10 at 40°C. Similar curves were obtained at 29°C and 51°C. A linear increase of the normalized mass uptake is observed as a function of  $t^{1/2}$ . The diffusion mechanism is Fickian from activity 0.1 up to activity 1. A fit with equation (2) gives excellent superposition with experimental data and provides the values of the diffusion coefficients for each water activity. In the case of PA6,6, for which non-Fickian diffusion was observed in liquid water, the DVS experiment gave the expected Fickian diffusion mechanisms for low activities, as illustrated in Figure 7(c). However, a change occurred around activity 0.7, at which point the slightly sigmoidal shape of the curve suggests that the condition of quasi-equilibrium is no longer fully satisfied (Figure 7(d)), or that water diffusion is intrinsically anomalous. An estimate of the diffusion coefficients can still be provided by the fit with equation (2). The same type of behavior was obtained at 29, 35 and 51°C.

The variation of the diffusion coefficients as a function of activity and temperature is shown in Figure 8 for both polyamides. It is observed that diffusion coefficients are not constant. They vary slightly in PA6,10, increasing by a factor 2 at most. In PA6,6, diffusion coefficients are much more dependent on activity, increasing by a factor about 5. A concentration dependent diffusion coefficient is one of the origins of non-Fickian diffusion mechanisms,<sup>42</sup> which might explain the sigmoidal sorption profile of water in PA6,6.

Moreover, Figure 8 illustrates that water diffusion is faster in PA6,10 than in PA6,6 at the same experimental temperature, especially at low activities. As the activity increases, the values of the diffusion coefficients in PA6,6 approach those in PA6,10. The experimental temperatures were also chosen so as to have equivalent  $T - T_g = 24^\circ\text{C}$ , as is the case for PA6,6 at 40°C and PA6,10 at 29°C or  $T - T_g = 13^\circ\text{C}$ , as is the case for PA6,6 at 51°C and PA6,10 at 40°C. As it will be highlighted in the next section, the glass transition temperature of the water-polyamide systems varies rapidly as water is absorbed so this initial condition of equivalent mobility of the polymer chains is no longer valid. Moreover, it can be noticed that diffusion coefficients are slightly higher in PA6,10 than in PA6,6 for the two equivalent

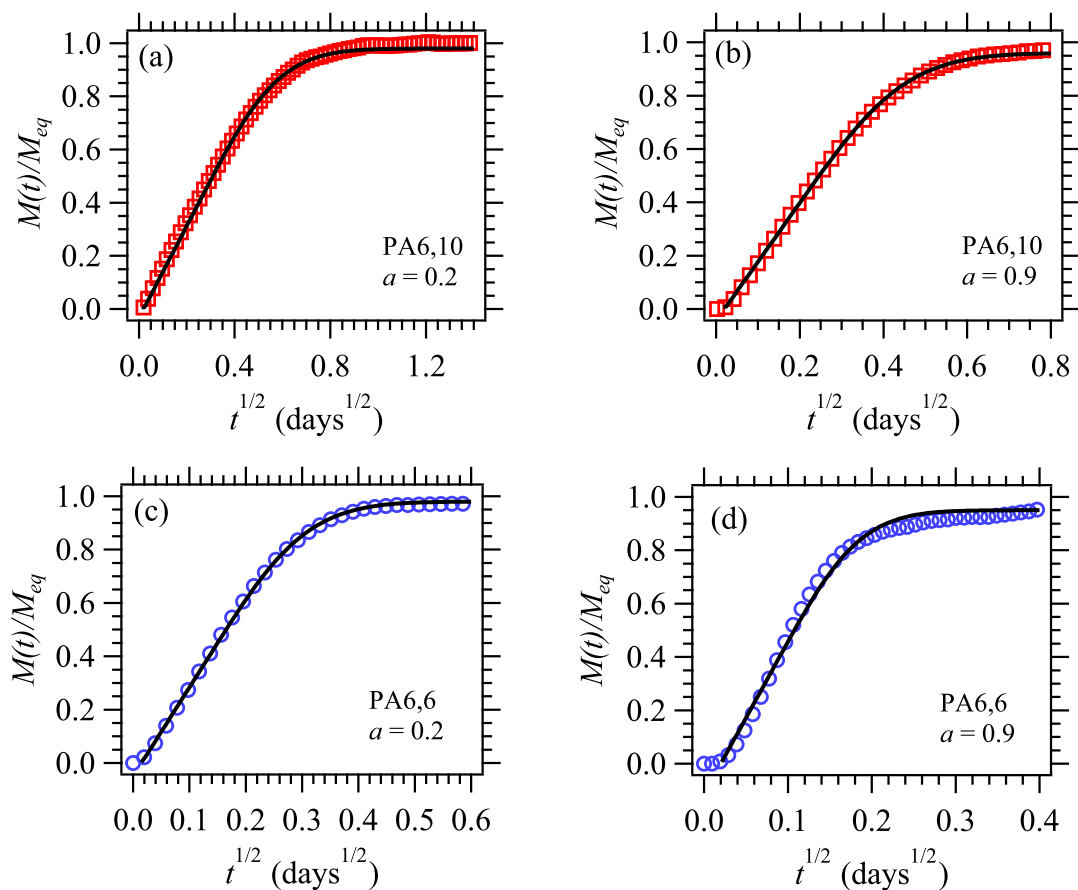


Figure 7: Experimental data and Fickian fits for the normalized mass increase as a function of  $t^{1/2}$  for water sorption in PA6,10 at 40°C and at activities 0.2 (a) and 0.9 (b); in PA6,6 at 40°C and at activities 0.2 (c) and 0.9 (d). Symbols are experimental points and lines are Fickian fits.

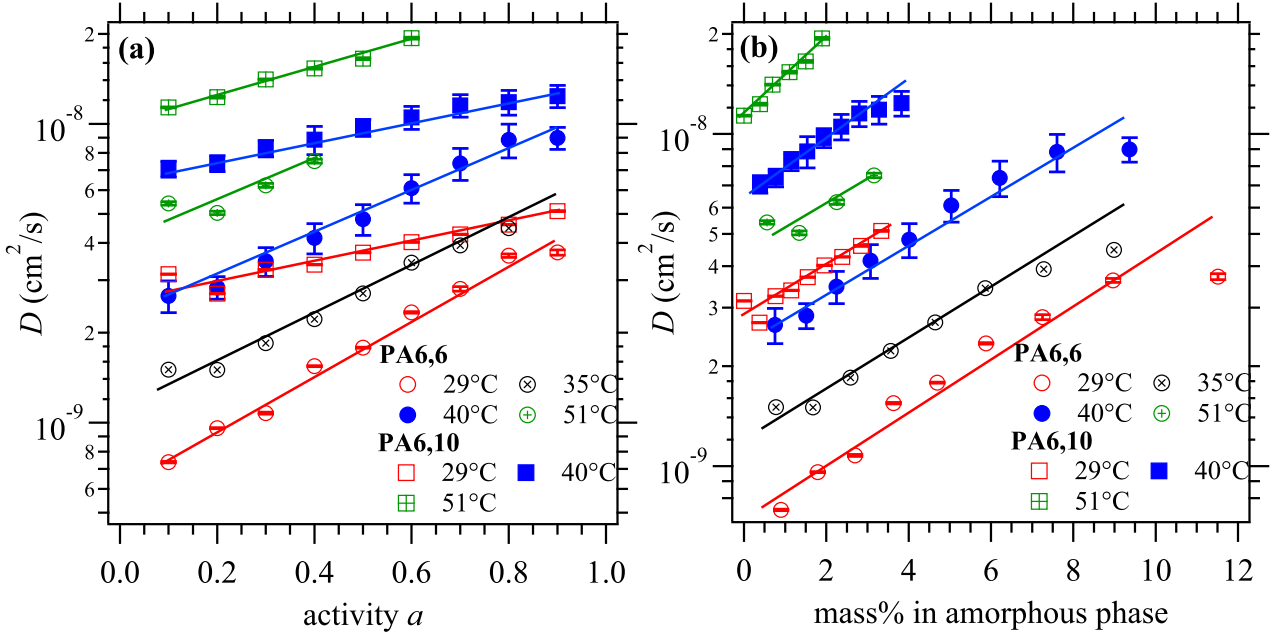


Figure 8: Variation of diffusion coefficients of water in PA6,6 and PA6,10 at different temperatures as a function of (a) water activity and (b) water intake in the amorphous phase. Lines are guides for the eye.

values of  $T - T_g$ .

### 3.3 $\alpha$ relaxations of water-polyamide systems

Anomalous or non-Fickian effects might be related to the influence of the evolving polymer mobility on diffusion or to the internal stresses (swelling) exerted as diffusion proceeds.<sup>42,46</sup> Since water decreases the glass transition temperature of polyamide,<sup>2,3</sup> it is interesting to study if there is a correlation between diffusion and the mobility of polymer chains.

To begin with, the glass transition temperatures  $T_g$  of the two polyamide-water systems were measured by Differential Scanning Calorimetry (DSC) at intermediate water mass uptakes corresponding to different activity values (Figure 9). As illustrated before by the sorption isotherms (Figure 6(b)), PA6,10 absorbs less water than PA6,6 in the activity range 0.1 to 0.9. The overall decrease in the glass transition temperature is thus smaller in PA6,10/water system at equilibrium than in PA6,6/water ( $-50^\circ\text{C}$  compared to  $-80^\circ\text{C}$ , respectively).

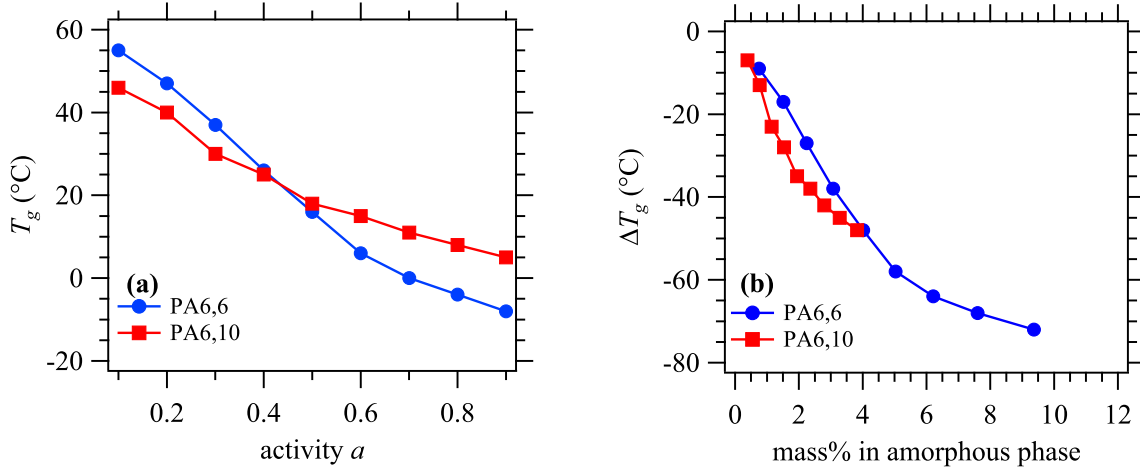


Figure 9: Shift in the glass transition temperature  $T_g$  measured by DSC in PA6,6 and PA6,10 as a function of (a) water activity and (b) water mass intake.

More detailed information on the polymer mobility can be obtained by dielectric spectroscopy. This technique gives access to the characteristic times of the polymer relaxations as a function of temperature. The  $\alpha$  relaxation in dielectric spectroscopy is associated to the glass transition so the  $\alpha$  relaxation times give an indication about the polymer mobility. The glass transition temperature measured by DSC can be added to these data by considering that the equivalent relaxation time in DSC measurements is approximately 100 seconds.<sup>36</sup> The relaxation times were measured for the dry and water equilibrated films with saturated salt solutions (activity 0.5, 0.75 and 0.84, Figure 10(a)).

The  $\alpha$  relaxation times as a function of temperature for both the dry (activity  $a = 0$ ) and liquid-water equilibrated ( $a = 1$ ) polyamide can be fitted by a Vogel-Fulcher-Tammann (VFT) equation (equation 1), which can be rewritten as:

$$\frac{1}{T} = \frac{1}{T_0 + \frac{A_{VFT}}{\ln(\tau/\tau_0)}} \quad (3)$$

where the VFT parameters  $T_0$ ,  $A_{VFT}$  and  $\tau_0$  depend on the activity. It was observed that the relaxation times for intermediate activities could be obtained by an interpolation method based on the position of the data points for DSC glass transition temperature ( $\ln \tau \simeq 4.6$ )

and their distances to the dry and liquid-water equilibrated polyamide VFT curves  $\ln \tau$  as a function of  $1/T$ . Based on the notations in Figure 10a, this semi-empirical interpolation method is given by Equation 4:

$$\frac{1}{T(a)} = \frac{x}{x+y} \frac{1}{T(a=1)} + \frac{y}{x+y} \frac{1}{T(a=0)} \quad (4)$$

where all temperatures correspond to the same value of  $\ln \tau$  and  $x$  and  $y$  are the differences between the inverse  $1/T_g$  of the polymer with water at activity  $a$  and  $1/T_g$  of the dry and water equilibrated polymer respectively. Equation 4 is analogous to the Fox-Flory mixing rule for the  $T_g$  of miscible blends.<sup>47</sup> It is an experimental finding here that the  $\alpha$  relaxation times for the systems equilibrated at intermediate water activities are well described by equation 4. Indeed, in Figure 10(a) it is observed that the dashed lines obtained from equation 4 superimpose over the experimental relaxation times represented by the markers, for the three intermediate activities. Equation 4 expresses the fact that the  $T_g$  of polyamide/water systems vs. activity curve (as shown in Figure 9) is independent of the frequency of the measurement.

The DSC glass transition temperature was available for all intermediate activities between 0.1 and 0.9. Therefore, the VFT curves for the  $\alpha$  relaxation times vs temperature at intermediate activities from 0.1 to 0.9 were estimated based on this interpolation method using equation 4. Finally, from the set of interpolated curves (as shown in Figure 10(b)), the relaxation time as a function of activity at a given experimental temperature was obtained by taking the intersections of the experimental temperature (vertical straight line Figure 10(b)) and of the interpolated relaxation time curves (Figure 10(b)).

The characteristic relaxation times  $\tau_\alpha$  of PA/water systems at different temperatures are illustrated in Figure 11(a) and (b) as a function of water mass intake in the polyamide amorphous phase. First of all, it can be noticed that  $\alpha$  relaxation times decrease when the water concentration increases, which is in agreement with polyamide being plasticized

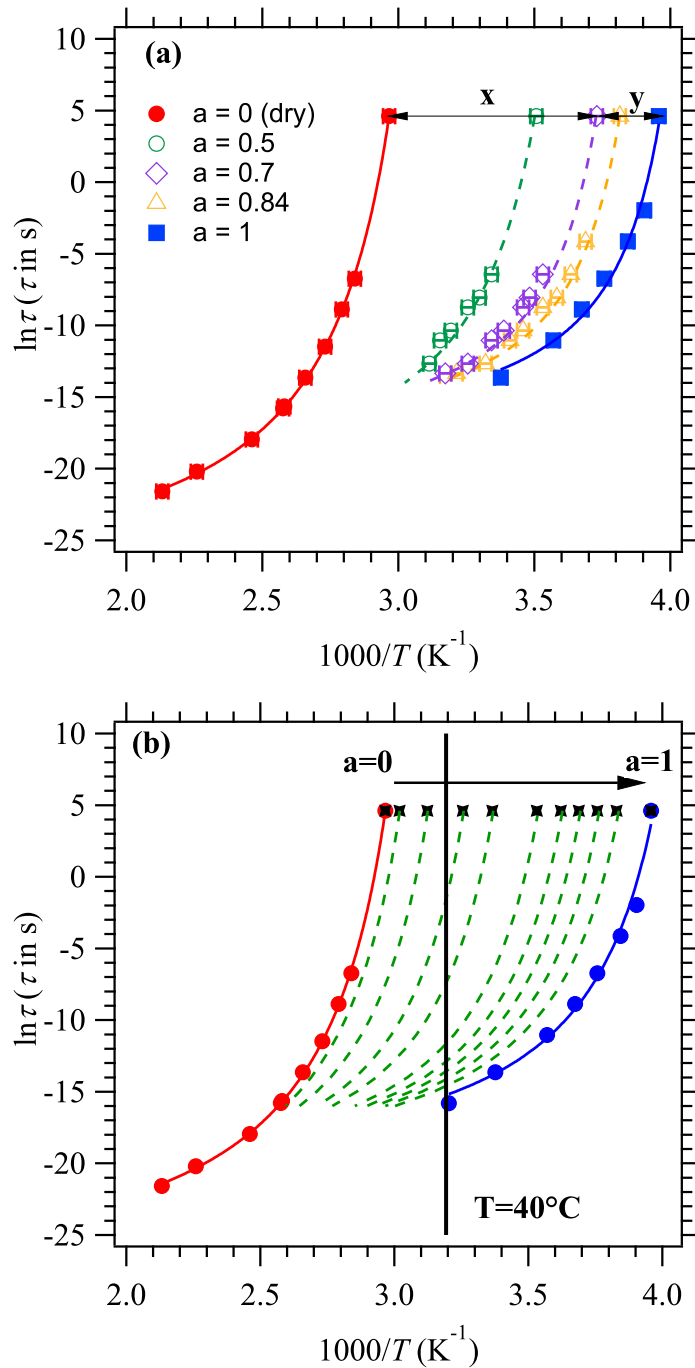


Figure 10: (a) Experimental  $\alpha$  relaxation times obtained from  $\epsilon''_{dielec}$  isochrones (markers), VFT fits (solid lines) and interpolation results (dashed line) for dry and water equilibrated ( $a = 0.5, 0.75, 0.84$  and 1) PA6,6; (b) Set of interpolated curves for all DVS intermediate activities and intersection with experimental temperature  $40^\circ C$ . Black markers correspond to the DSC measured  $T_g$ 's of polyamide/water systems at intermediate activities.

by water. Also, as expected, the  $\alpha$  relaxation times of the polymer systems decrease when temperature increases. At equivalent water intake,  $\tau_\alpha$  of the PA6,10/water systems are shorter than  $\tau_\alpha$  of the PA6,6/water systems for all temperatures.

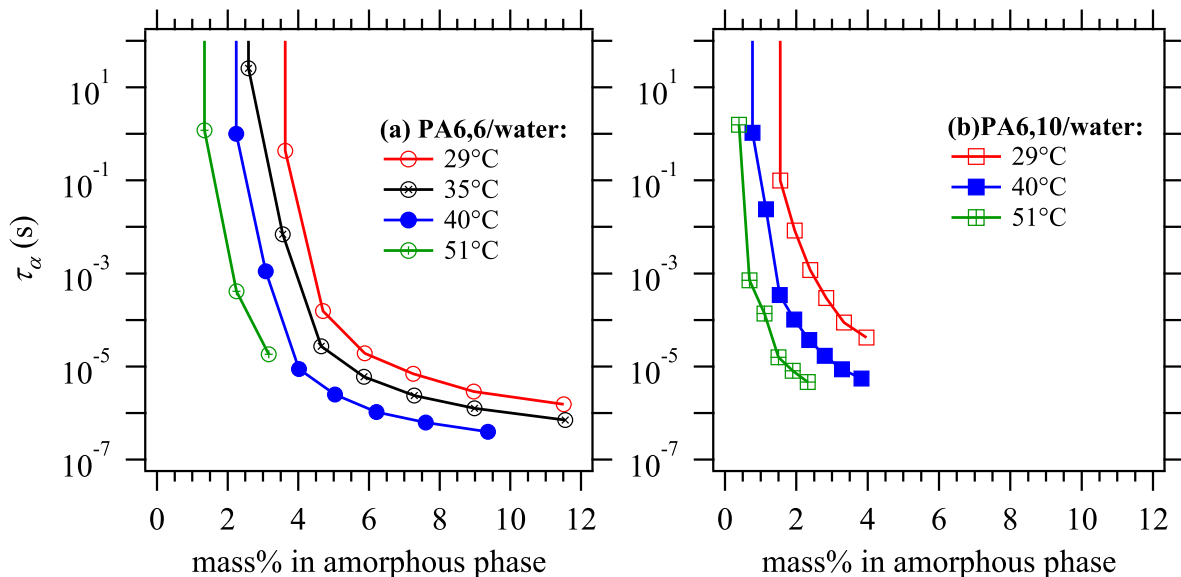


Figure 11:  $\alpha$  relaxation times in logarithmic scale for (a) PA6,6/water and (b) PA6,10/water systems as a function of water intake in the amorphous phase at different temperatures. Lines are guides for the eye.

### 3.4 $\beta$ relaxations of water-polyamide systems

As mentioned in Section 2.5, the relaxation processes in the  $\beta$  region are also strongly affected by the presence of water (see Figures 3 and 12). The corresponding relaxation maps for the  $\beta_w$  relaxation in the presence of water in both polymers are shown in Figure 12. For both polymers, the characteristic  $\beta_w$  relaxation times at a constant temperature become shorter in presence of water.

The variation of the relaxation times can be fitted with an Arrhenius equation  $\tau = \tau_0 \exp [E/RT]$  and gives the parameters listed in Table 1.

The activation energy for a  $\beta$  secondary relaxation should be around 30-40 kJ/mol<sup>36</sup>. In this case, the activation energies are more than doubled and the values of  $\tau_0$  have no physical

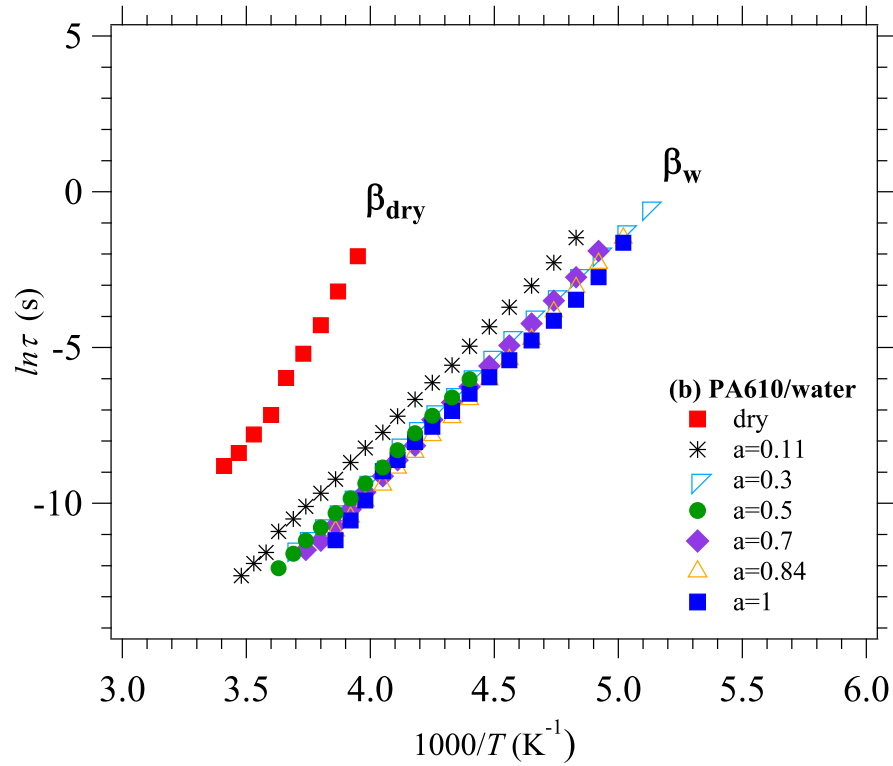
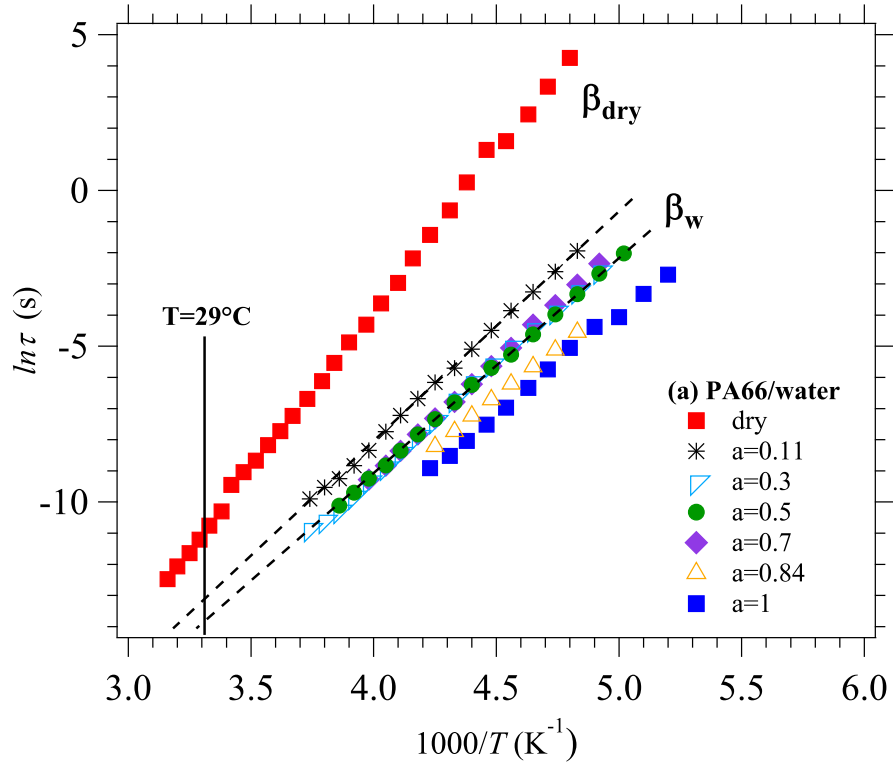


Figure 12: Relaxation maps for the  $\beta$  relaxations for (a)PA6,6 and (b)PA6,10 for various water activities. The dotted lines in figure (a) are the Arrhenius fits of the relaxation times, which can be extrapolated to obtain the characteristic  $\beta$  relaxation times at DVS experimental temperatures (e.g. 29°C)



Table 1: Arrhenius parameters from the  $\beta$  relaxation maps of PA6,10 and PA6,6 at various water activities shown in Figure 12.

	PA6,6		PA6,10	
activity	$E_a$ (kJ/mol)	$\tau_0$ (s)	$E_a$ (kJ/mol)	$\tau_0$ (s)
0 (dry)	85	3.6E-20	103	4.3E-23
0.11	62	2.2E-17	66	5.2E-18
0.3	60	3.0E-17	65	2.7E-18
0.5	58	7.9E-17	65	2.3E-18
0.7	62	1.2E-17	68	4.5E-19
0.84	54	2.9E-16	67	6.3E-19
1	54	1.2E-16	64	2.7E-18

relevance. This is an indication that the  $\beta$  relaxation in polyamide is not a simple process involving the rotation of a single amide group or the dissociation of a single hydrogen bond. The complexity could be due to cooperative movements of the amide groups.

The Arrhenius equation and the parameters in Table 1 were used in order to extrapolate the characteristic  $\beta_w$  relaxation times at the experimental DVS temperatures (see extrapolation in Figure 12 (a)). The variation of the characteristic  $\beta_w$  relaxation time as a function of water content in both polymers at DVS experimental temperatures are shown in Figure 13. **The obtained values are considered to be representative of the local chain dynamics of hydrogen bonded amide groups. Although  $\beta$  relaxation times approach  $\alpha$  relaxation times in presence of water, the two processes are still sufficiently separated to be studied individually.** As in the case of the  $\alpha$  relaxation,  $\beta$  relaxation times decrease when the water content or temperature increases. The same order of magnitude, 0.1 to 1 microseconds, is observed in both polymers.

## 4 Discussion

### 4.1 Sorption isotherms

Before addressing the question of diffusion mechanisms, which is the core of this paper, it is interesting to recall some basic considerations about water sorption. Indeed, analyzing

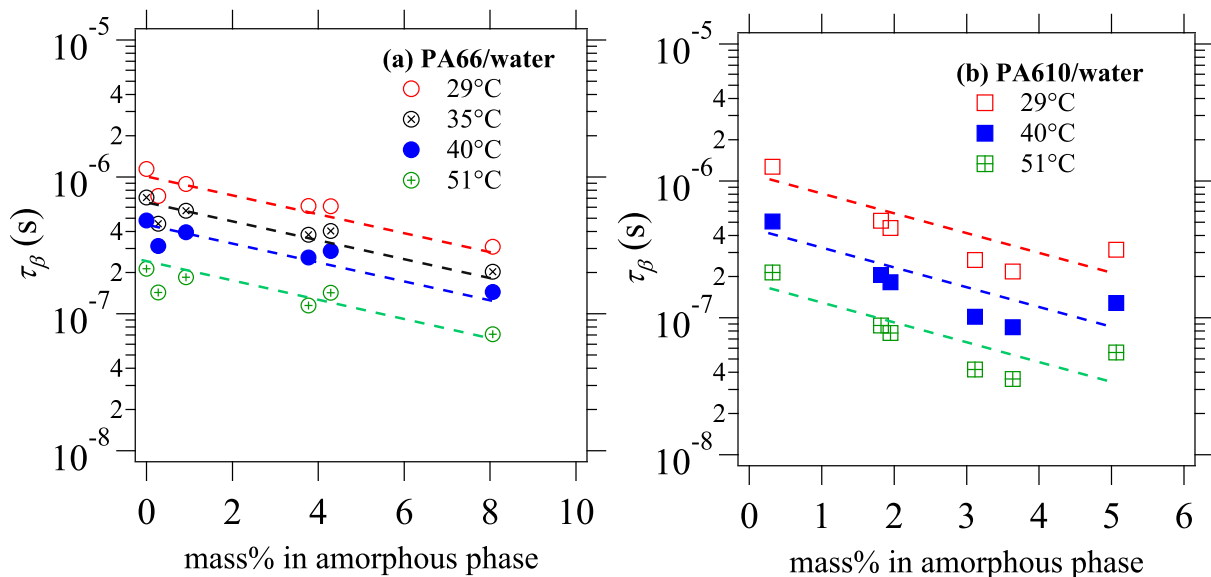


Figure 13: Characteristic  $\beta$  relaxation times as a function of water uptake in the amorphous phase of (a) PA6,6 and (b) PA6,10 corresponding to DVS experimental temperatures. Lines are guides for the eye.

sorption isotherms already gives some pieces of information on the effect of water on the polymer matrix.

Since the two polymers were prepared by different processing methods, the comparison between them is not straightforward. Indeed it is well established that morphology and phase composition are influenced by processing and thermal history of semi-crystalline polymers.<sup>21,22,24,27,48,49</sup> For the diffusion and polymer relaxation investigation, the two polyamides were studied independently and the same conclusions were reached. For sorption isotherms, each matrix was analyzed individually as well.

Measured sorption isotherms are in agreement with those reported in the literature.<sup>2,5,7,9</sup> The upward curvature of water sorption isotherms might be associated to the swelling of the matrix or to the existence of water clusters.<sup>2,5,50</sup> The Flory-Huggins model for binary mixtures takes into account the swelling of the matrix and fits the experimental data with equation (5)<sup>51</sup> :

$$\ln a = \ln \varphi + (1 - \varphi) + \chi(1 - \varphi)^2 \quad (5)$$

where  $\varphi$  is the volume fraction of solvent in the polymer and  $\chi$  is the Flory-Huggins interaction parameter. Equation (5) provides an excellent fit for all experimental data and the obtained  $\chi$  values are 1.5 for PA6,6 at 29°C, 1.63 for PA6,6 at 40°C and 2.32 for PA6,10 at 29 and 40°C. A higher Flory-Huggins parameter in PA6,10 suggests that water is a worse solvent for PA6,10 than for PA6,6, which is in accordance with PA6,10 being more hydrophobic. The value of the interaction parameter  $\chi$  can alternatively be estimated with equation 6:<sup>52</sup>

$$\chi = \frac{(\delta_i - \delta_j)^2}{RT} \sqrt{v_i v_j} \quad (6)$$

where  $\delta$  is the Hildebrand solubility parameter,  $R$  is the gas constant,  $T$  is the temperature and  $v$  is the molar volume of each specie. The reported values for Hildebrand solubility parameters are 27.8 MPa<sup>1/2</sup> for PA6,6,<sup>53,54</sup> 26 MPa<sup>1/2</sup> for PA6,10 (calculated with group contribution<sup>55</sup>) and 48 MPa<sup>1/2</sup> for water as a pure liquid.<sup>52</sup> Based on equation (6) and the reported values of solubility parameters, the values of the Flory interaction parameter  $\chi$  would be 5.05 for PA6,6/water and 6.75 for PA6,10/water at 40°C. These values are much larger than the  $\chi$  values obtained from fitting the sorption isotherms. Experimental water intake is thereby much higher than predicted from the calculated  $\chi$  values. Moreover, in the Flory approach, the water intake should increase with temperature, entropy being the driving force for sorption. However, it is found that the water intake either decreases (PA6,6) or is roughly constant (PA6,10) as a function of temperature. This suggests that sorption enthalpy is more likely to be the driving force for sorption, and therefore, that an enthalpy-driven model with specific sorption sites is more appropriate.

The Guggenheim, Anderson and De Boer (GAB)<sup>56-58</sup> model assumes the existence of preferential sorption sites (in the present case amide groups). The model allows sorption in several layers and differentiates between the water molecules from the first sorbed layer and the ones from the additional layers. The sorption isotherms can be fitted with equation (7)

(fit shown in Figure 6(b)):

$$M(a) = \frac{M_m A C a}{(1 - A a)(1 - A a + A C a)} \quad (7)$$

where  $M(a)$  is the solvent uptake at activity  $a$ ,  $M_m$  is the solvent content corresponding to saturation of all primary absorption sites by one solvent molecule (monolayer),  $C$  is the Guggenheim constant and represents the difference in the adsorption energy for the first layer and the other successive layers and  $A$  is a factor correcting the properties of the multilayer molecules with respect to the bulk liquid.

The GAB parameters resulting from the fits are:  $M_m = 4.99\%$ ,  $A = 0.71$ ,  $C = 2.74$  (PA6,6 at 29°C);  $M_m = 4.99\%$ ,  $A = 0.72$ ,  $C = 2.58$  (PA6,6 at 35°C);  $M_m=4.99\%$ ,  $A=0.65$ ,  $C=2.4$  (PA6,6 at 40°C) and  $M_m=3.61\%$ ,  $A =0.47$ ,  $C=2.26$  (PA6,10 at 29°C),  $M_m=3.61\%$ ,  $A =0.46$ ,  $C=2.39$  (PA6,10 at 40°C) and  $M_m=3.61\%$ ,  $A =0.48$ ,  $C=2.11$  (PA6,10 at 51°C).

The values of the GAB parameters are in agreement with the literature.<sup>2</sup> The obtained solvent content in the first layer  $M_m$  is 5% in PA6,6 and 3.6% in PA6,10, which is close to the 1.25 ratio predicted by the difference in amide groups density. The Guggenheim constants  $C$  and constant  $A$  have close values in the two polyamides, indicating that there is little difference in the adsorption energy of a water molecule in PA6,6 or in PA6,10.

The GAB parameters can also be used to estimate the size of the water clusters (Mean Cluster Size,  $MCS$ ) with the following equation (8):<sup>59</sup>

$$MCS = -(1 - \varphi) \left[ \frac{\varphi}{M_m C} (-2 + 2Aa - 2ACa + C) - 1 \right] \quad (8)$$

The equation provides a  $MCS$  of 2 for water in PA6,6 at 29°C, 1.7 for water in PA6,6 at 40°C and 1.3 for water in PA6,10 at 29 and 40°C. These values are in accordance with literature data for PA6,6<sup>2,5</sup> and with results of molecular dynamic simulations<sup>60</sup>. A low  $MCS$  value of 1.3 for water in PA6,10, as well as the linear shape of the sorption isotherm suggest that water does not form clusters in PA6,10. Altogether, this indicates that water

is distributed in polyamide down to molecular size (or length scale) or nearly (cluster size 1.5-2) and does not form nanodomains (ordered or not) like for example in lyotropic systems (surfactant/water mixtures). This implies that diffusion will be isotropic, not affected by structuration at nanometer scale. Note however that diffusion is affected by the presence of crystallites.

## 4.2 Correlation between water diffusion and polymer relaxation mechanisms

The correlation between water diffusion and polyamide relaxations is now discussed. The diffusion coefficients and relaxation times of polyamide/water systems were measured for different water activities/intakes. For a given temperature, the diffusion coefficient can therefore be plotted as a function of the relaxation times as the water concentration or activity varies. This is first done for the  $\alpha$  relaxation in Figure 14.

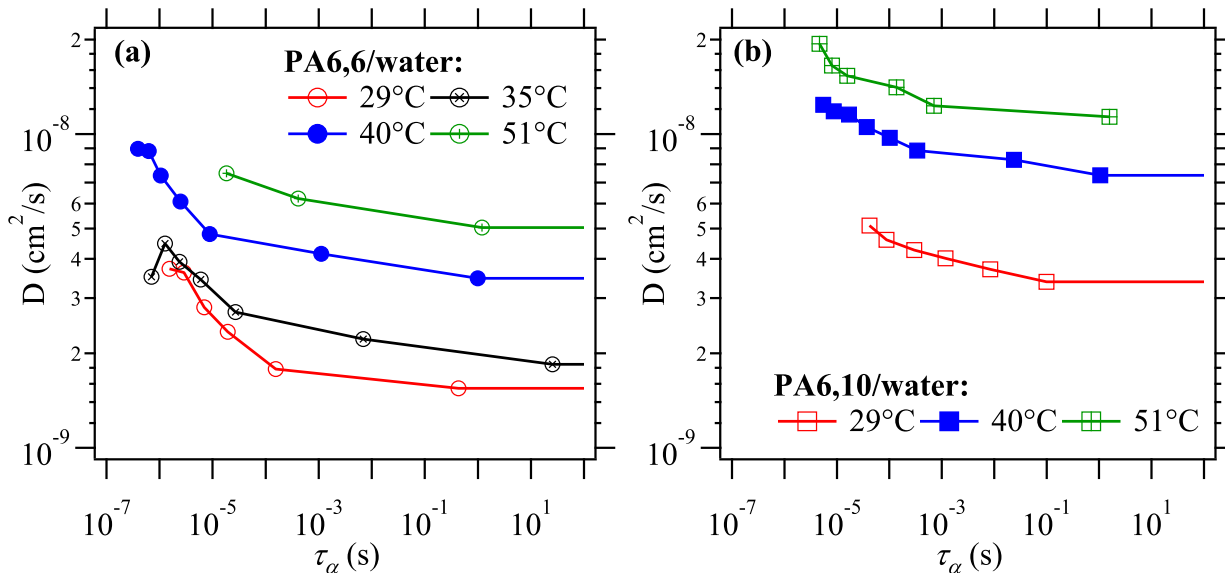


Figure 14: Water diffusion coefficient  $D$  as a function of the  $\alpha$  relaxation times  $\tau_\alpha$  at different temperatures for (a) PA6,6/water and (b) PA6,10/water systems.

At each temperature, diffusion coefficients vary by a factor 2 to 5, whereas  $\tau_\alpha$  relaxation times vary over 7 orders of magnitude. Thus, there is a huge difference between the mag-

nitude of the variation of diffusion coefficients and  $\tau_\alpha$  as a function of water content: the two processes seem to follow distinct timescales. These results are in agreement with NMR studies that showed a few percentages of water already penetrate in polyamide before the plasticization sets in.<sup>28</sup> The authors concluded on the existence of a plasticization lag, which also suggests that plasticization and diffusion are not directly correlated. In addition, this set of data gives access to the variation of the diffusion coefficients as a function of temperature, for a constant characteristic rate of segmental motions of the matrix. The variation of  $D$  with temperature can be represented at constant  $\tau_\alpha$  of the matrix (Figure 15).

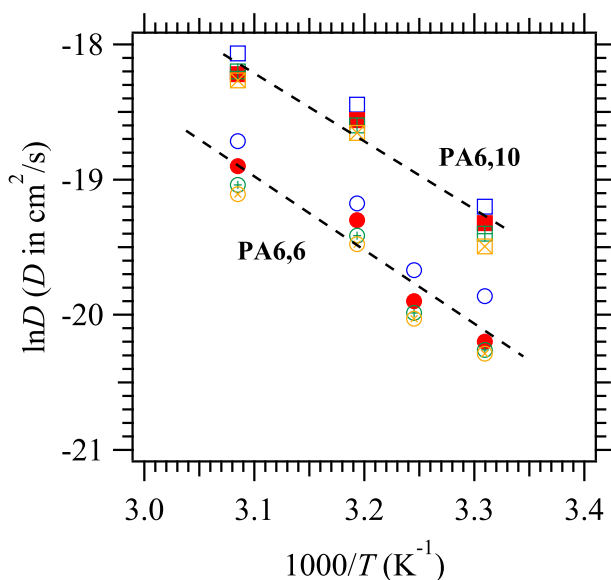


Figure 15: Variation of diffusion coefficients as at different temperatures for constant  $\tau_\alpha$  relaxation times. PA6,10 (squares):  $\tau_\alpha = 10^{-4}$  s (blue),  $10^{-3}$  s (red),  $10^{-2}$  s (green),  $10^{-1}$  s (orange); PA6,6 (circles):  $\tau_\alpha = 2 \times 10^{-5}$  s (blue),  $10^{-3}$  s (red),  $10^{-1}$  s (green), 1 s (orange).

Figure 15 shows that the variation of the diffusion coefficients may reasonably be considered to be Arrhenian with temperature, for each different relaxation times of the polyamide/water system. The curves can be fitted with an Arrhenius law to give access to an activation energy for diffusion. The fits are presented in Figure 15 as dashed lines. The associated activation energies are  $46 \pm 10$  kJ/mol for PA6,6 and  $43 \pm 10$  kJ/mol for PA6,10. The activation energy for diffusion seems to be independent of the relaxation state of the polymer. Along with the distinct timescales of the diffusion and relaxation processes, this would suggest that

there is no direct correlation between the two phenomena.

The activation energies for diffusion are only slightly different in PA6,6 and PA6,10, suggesting that water diffusion mechanisms at molecular scale are similar. **Note, however, that activation energies for diffusion of various gas and water molecules are found to be of the order 30-60 kJ/mol in a wide variety of amorphous or semi-crystalline polymers.<sup>45</sup> Thus, such values for the activation energy do not allow discriminating a particular mechanism per se.**

At a molecular level, it is then interesting to investigate the correlation of diffusion to local movements, more specifically the  $\beta$  relaxation. This secondary relaxation combines conformational changes around amide groups and hydrogen bond relaxation. There are several concordant indications that diffusion may be controlled by the lifetime of hydrogen bonds, that is, by the local environment around a water molecule being hydrogen-bound to an amide group. First, in polyamides, strong interactions exist between water molecules and the amide preferential sorption sites, as already mentionned before. Another argument is the fact that diffusion coefficients are only little affected by the huge variation of the polymer matrix  $\alpha$  relaxation time, as described above.

Following the same procedure as for the  $\alpha$  relaxation, the water diffusion coefficients are plotted as a function of the high frequency  $\beta$  relaxation times for various water activities and various temperatures in both PA6,6 and PA6,10 in Figure 16.

In this case, the variations of the diffusion coefficients and  $\beta$  relaxation times are of the same order of magnitude. To assess the contribution of the  $\beta$  relaxation and hydrogen bonding to the diffusion process, the diffusion characteristic time can be compared to the  $\beta$  relaxation time and the lifetime of a hydrogen bond. Assuming that water molecules diffuse between neighboring amide groups, the characteristic time for diffusion is proportional to the square length of distance over the diffusion coefficient. Based on elementary density arguments, the average distance  $d$  between amide groups can be evaluated to approximately 0.7 nm in PA6,6 (in agreement with simulation results<sup>61</sup>) and 0.8 nm in PA6,10, due to the

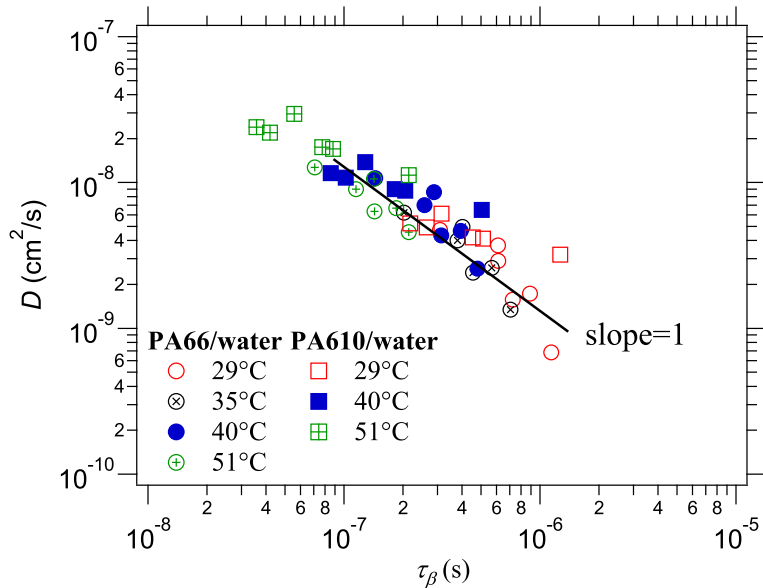


Figure 16: Water diffusion coefficient  $D$  as a function of the characteristic  $\beta$  relaxation times at different temperatures for PA6,6/water and PA6,10/water systems. Each series of points corresponds to a given  $T$ , each point in a series corresponds to a given water activity. The line with a slope of 1 is a guide for the eyes.

additional methylene groups. For both polymers, the calculated characteristic diffusion times  $t_D \approx d^2/2D$  range from  $10^{-7}$  to  $10^{-6}$  s. Estimations for water-amide group interaction energy can be found in the literature,<sup>10,62</sup> based on ab-initio calculations for peptide-water systems in vacuum. The interaction energy thus obtained is approximately 30-35 kJ/mol. In a polymer environment, this interaction energy might be different because of hydrophobic contributions. Taking the relaxation time of a hydrogen bond as Arrhenian  $\tau = \tau_0 \exp[E/RT]$  with a characteristic  $\tau_0$  of  $10^{-12}$  to  $10^{-10}$  s<sup>-1</sup> and an activation energy  $E$  of 30-35 kJ/mol,<sup>11</sup> the lifetime of a hydrogen bond is estimated between  $10^{-7}$  and  $10^{-5}$  s in the experimental temperature range.

Note that  $\beta$  relaxation has an apparent activation energy of the order of 60 kJ/mol (as mentioned before), which indicates that it involves more complex, perhaps more cooperative processes than just the rotation of an amide group or breaking of one hydrogen bond. In any case, the characteristic  $\beta$  relaxation times are found experimentally in the range  $10^{-7}$  and  $10^{-6}$  s, as illustrated in Figure 16. Therefore, the characteristic diffusion time, the  $\beta$



relaxation time and the lifetime of the hydrogen bond are of the same order of magnitude, which suggests that diffusion of water in polyamide may indeed be limited by the departure of the water molecule from the amide sorption site. Consequently, the hopping in between sites should be very fast.

Thus, the values of the diffusion coefficients themselves seem to be compatible with a very simple picture in which diffusion would be controlled by hopping from one amide group to the neighboring one.

Since the two polyamides studied here have not been processed with the same method, a direct comparison would somehow be hazardous. The type of mechanism suggested above would predict a faster diffusion through a polymer that has sorption sites separated by longer distances (if  $t_D$  is similar, then  $D \sim \frac{d^2}{2t_d}$  is higher when  $d$  is higher), which is in accordance with the experimental observation that water diffusion is faster in PA6,10 than in PA6,6, either we compare at the same temperature or at equivalent  $T - T_g$ . Measured diffusion coefficients in PA6,10 are 2 to 4 times larger than in PA6,6. However, this ratio is significantly larger than predicted from the ratio of average distances between amide groups in both polymers. This difference might arise from the samples microstructures. The crystalline fraction is larger in PA6,6 than in PA6,10 (38% compared to 23%). Indeed, crystallites,<sup>63,64</sup> as well as the rigid amorphous phase, may strongly affect diffusion coefficients. The measured diffusion coefficient  $D$  can be expressed by equation 9:

$$D = \frac{D^*}{\xi \beta_{imm}} \quad (9)$$

where  $D^*$  is the diffusion coefficient in the bulk amorphous polymer,  $\beta_{imm}$  is a chain immobilization factor that relates to the fraction of rigid amorphous phase and  $\xi$  is the tortuosity factor that accounts for the increased diffusion path in order to bypass crystallites.<sup>65</sup> One expression for the tortuosity factor proposed in the context of polymers nanocomposites with layered clay fillers of aspect ratio  $f$  is of the form  $\xi \simeq 1 + \frac{f}{6} X_c$ , where  $X_c$  is the volume fraction

of layered objects (taken to be here crystalline lamellae or lamellar stacks) and integration has been done over all possible lamella orientations.<sup>65,66</sup> With  $X_c$  varying from 23% to 38%, it is easy to explain the ratio between diffusion coefficients with reasonable values of the aspect ratio. Also, the chain immobilization factor should not be the same in the two polymers. Note again, that a direct comparison of diffusion coefficients between polyamides with different amide group densities would require a detailed control of the processing conditions and an extensive characterisation of the microstructure.

## 5 Conclusions

The diffusion of water in semi-crystalline polyamides (PA6,6 and PA6,10) was investigated. First, it was found that the diffusion of liquid water is apparently Fickian in PA6,10 and non-Fickian or anomalous in PA6,6. Then, in order to get a more detailed insight on diffusion mechanisms, a quasi-equilibrium experiment was set up to measure selectively the variation of the diffusion coefficient as a function of water activity/concentration at equilibrium.

It was thus shown that the diffusion coefficient of water in PA6,6 increases significantly as the water concentration increases, which accounts for the non-Fickian diffusion in this polymer. In PA6,10, this variation is much less pronounced, which supports an apparent Fickian diffusion.

Moreover, the polymer relaxation times associated to the glass transition ( $\alpha$  relaxation) and to the  $\beta$  secondary relaxation of the amorphous phase of the polyamides were measured or estimated as a function of temperature and water concentration by Broadband Dielectric Spectroscopy. The  $\alpha$  relaxation times decrease by several orders of magnitude, illustrating the polymer plasticization by water molecules. This variation (typically 6 orders of magnitude) is much more extensive than the variation of diffusion coefficients (a factor 2 to 5 at most) over the activity range from 0 to one, indicating that diffusion is not controlled primarily by the  $\alpha$  relaxation in polyamide. Conversely, the variation of the diffusion coef-

ficient with water concentration is coherent with that of the  $\beta$  relaxation time. The results are compatible with a diffusion process controlled by the hopping of water molecules between preferential adsorption sites (amide groups), with which they form hydrogen bonds.

## Acknowledgement

The authors thank Danielle Lamberet and Jean-Claude Le Thiesse (Solvay, Lyon) for their help with DVS measurements and Silvia Arrese-Igor (Centro de Fisica de Materiales, San Sebastian, Spain) for High Frequency Dielectric Spectroscopy measurements, funded by the European Soft Matter Infrastructure (ESMI) program (grant no. 262348). The Broadband Dielectric Spectrometer was funded by the GRAND LYON Metropolitan Council.

## References

- (1) Kohan, M. *Nylon Plastics Handbook*; Wilmington:Hanser, 1995.
- (2) Lim, L.; Britt, I.; Tung, M. *Journal of Applied Polymer Science* **1999**, *71*, 197.
- (3) Rios de Anda, A.; Fillot, L. A.; Rossi, S.; Long, D.; Sotta, P. *Polymer Engineering & Science* **2011**, *51*, 2129–2135.
- (4) Starkweather, H. *Journal of Applied Polymer Science* **1959**, *2*, 129.
- (5) Starkweather, H. *Macromolecules* **1975**, *8*, 476.
- (6) Garcia, D.; Starkweather, H. *Journal of Polymer science: Polymer Physics Edition* **1985**, *23*, 537–555.
- (7) Puffr, R.; Sebenda, J. *J. Polym. Sci. C* **1967**, *16*, 79–93.
- (8) Skirrow, G.; Young, K. *Polymer* **1974**, *15*, 771–776.
- (9) Auerbach, I.; Carnicom, M. *Journal of Applied Polymer Science* **1991**, *42*, 2417.

- (10) Jorgensen, W.; Swenson, C. *J. Am. Chem. Soc.* **1985**, *107*, 1489.
- (11) Camacho, W.; Hedenqvist, M. S.; Karlsson, S. *Polymer International* **2002**, *51*, 1366–1370.
- (12) Goudeau, S.; Charlot, M.; Vergelati, C.; Müller-Plathe, F. *Macromolecules* **2004**, *37*, 8072–8081.
- (13) Laurati, M.; Sotta, P.; Long, D. R.; Fillot, L. A.; Arbe, A.; Alegria, A.; Embs, J. P.; Unruh, T.; Schneider, G. J.; Colmenero, J. *Macromolecules* **2012**, *45*, 1676–1687.
- (14) Murthy, N. S. *Journal of Polymer Science: Part B: Polymer Physics* **2006**, *44*, 17631782.
- (15) Reimschuessel, H. K. *Journal of Polymer Science: Polymer Physics* **1978**, *16*, 12291236.
- (16) Murthy, N. S.; Stamm, M.; Sibilía, J. P.; Krimm, S. *Macromolecules* **1989**, *22*, 12611267.
- (17) Hedenqvist, M.; Gedde, U. *Prog. Polym. Sci.* **1996**, *21*, 299–333.
- (18) Flory, P. *Journal of the American Chemical Society* **1962**, *84*, 2857–2868.
- (19) Murthy, N. S.; Akkapeddi, M. K.; Orts, W. J. *Macromolecules* **1998**, *31*, 142–152.
- (20) Hutchison, J. L.; Murthy, N. S.; Samulski, E. T. *Macromolecules* **1996**, *29*, 5551–5557.
- (21) Litvinov, M.; Penning, J. P. *Macromolecular Chemistry and Physics* **2004**, *205*, 1721–1734.
- (22) Litvinov, V. M.; Persyn, O.; Miri, V.; Lefebvre, J. M. *Macromolecules* **2010**, *43*, 7668–7679.
- (23) Litvinov, V. M.; Koning, C. E.; Tijssen, J. *Polymer* **2015**, *56*, 406–415.

- (24) Adriaensens, P.; Pollaris, A.; Carleer, R.; Vanderzande, D.; Gelan, J.; Litvinov, V. M.; Tijssen, J. *Polymer* **2001**, *42*, 7943–7952.
- (25) Adriaensens, P.; Pollaris, A.; Rulkens, R.; Litvinov, V. M.; Gelan, J. *Polymer* **2004**, *45*, 2465–2473.
- (26) Reuvers, N.; Huinink, H.; Fischer, H.; Adan, O. *Macromolecules* **2012**, *45*, 1937–1945.
- (27) Reuvers, N.; Huinink, H.; Adan, O. *Macromolecular Rapid Communications* **2013**, *34*, 949–953.
- (28) Reuvers, N.; Huinink, H.; Adan, O. *Polymer* **2015**, *63*, 127–133.
- (29) Nguyen, T. Q. *J. Liq. Chrom. & Rel. Technol* **2001**, *24*, 2727–2747.
- (30) Fontana, A. J. *Water Activity in Foods*; Blackwell Publishing Ltd, 2008; pp 391–393.
- (31) Laurati, M.; Arbe, A.; Rios de Anda, A.; Fillot, L. A.; Sotta, P. *Polymer* **2014**, *55*, 2867–2881.
- (32) McCrum, N.; Read, B.; Williams, G. *Anelastic and Dielectric Effects in Polymeric Solids*; Wiley, 1967.
- (33) Le Huy, H.; Rault, J. *Polymer* **1994**, *35*, 136.
- (34) Laredo, E.; Hernández, M. *J. Polym. Sci. Part B: Polym. Phys.* **1997**, *35*, 2879.
- (35) Laredo, E.; Grimau, F.; Sánchez, F.; A. Bello, A. *Macromolecules* **2003**, *36*, 9840.
- (36) Kremer, F.; Schönhals, A. *Broadband Dielectric Spectroscopy*; Springer, 2003.
- (37) Vogel, H. *Phys Z* **1921**, *22*, 645.
- (38) Fulcher, G. *Journal of the American Ceramic Society* **1923**, *8*, 339.
- (39) Tammann, G.; Hesse, W. *Z Anorg Allg Chem* **1926**, *156*, 245.

- (40) Alfrey, T.; Gurnee, E. *Journal of Polymer Science Part C* **1966**, *12*, 249–261.
- (41) Yamamoto, U.; Schweizer, K. *Macromolecules* **2015**, *48*, 152–163.
- (42) Crank, J. *The Mathematics of Diffusion, 2nd edition*; Clarendon Press - Oxford, 1975.
- (43) Berens, A.; Hopfenberg, H. *Polymer* **1978**, *19*, 489–496.
- (44) Hedenqvist, M.; Gedde, U. *Polymer* **1999**, *40*, 2381–2393.
- (45) Brandrup, J.; Immergut, E. H.; Grulke, E. A. *Polymer Handbook, 4th edition*; 2003.
- (46) Klopffer, M.; Flaconnèche, B. *Oil & Gas Science and Technology Rev. IFP* **2001**, *56*, 223–244.
- (47) Fox, T. *Bull. Am. Phys. Soc.* **1956**, *1*, 123.
- (48) Lasoski, S. W.; Cobbs, W. H. *Journal of Polymer Science* **1959**, *36*, 21–33.
- (49) Rastogi, S.; Terry, A. E.; Vinken, E. *Macromolecules* **2004**, *37*, 8825–8828.
- (50) Zimm, B. H.; Lundberg, J. L. *Journal of Physical Chemistry* **1956**, *60*, 425.
- (51) Flory, P. *Principles of polymer chemistry*; Cornell University Press: Ithaca, 1953.
- (52) Barton, A. F. M. *A. F. M. Barton, Handbook of Solubility Parameters and Other Cohesion Parameters, 1983*; CRC Press: Boca Raton, FL., 1983.
- (53) Patrick, R. *Treatise on Adhesion and Adhesives Vol. 1*; Marcel Dekker: New York, 1967.
- (54) Vandenburg, H.; Clifford, A.; Bartle, K.; Carlson, R.; Carroll, J.; Newton, I. *Analyst* **1999**, *124*, 1707–1710.
- (55) Stefanis, E.; Panayiotou, C. *Int J Thermophys* **2008**, *29*, 568–585.
- (56) Anderson, R. *Journal of the American Chemical Society* **1946**, *69*, 686–691.

- (57) de Boer, J. *The dynamic character of adsorption*; Oxford Clarendon Press, 1953; pp 61–81.
- (58) Guggenheim, E. *Oxford Clarendon Press* **1966**, 186–206.
- (59) Zhang, Z.; Britt, I. J.; Tung, M. A. *Journal of Polymer Science, Part B: Polymer Physics* **1999**, *37*, 691–699.
- (60) Eslami, H.; Müller-Plathe, F. *The Journal of Physical Chemistry B* **2011**, *115*, 9720–9731.
- (61) Eslami, H.; Müller-Plathe, F. *The Journal of Physical Chemistry C* **2013**, *117*, 5249–5257.
- (62) Sun, C.-L.; Jiang, X.-N.; Wang, C.-S. *Journal of Computational Chemistry* **2009**, *30*, 2567–2575.
- (63) Michaels, A.; Parker, R. *Journal of Polymer Science* **1959**, *41*, 53–71.
- (64) Michaels, A.; Bixler, H. *Journal of Polymer Science* **1961**, *50*, 413–439.
- (65) Bharadwaj, R. K. *Macromolecules* **2001**, *34*, 9189–9192.
- (66) Nielsen, L. E. *J. Macromol. Sci., Chem.* **1967**, *A1*, 929–942.

## 6 For Table of Contents use only

### Investigation of water diffusion mechanisms in relation to polymer relaxations in polyamide

*Florentina-Maria Preda, Angel Alegría, Anthony Bocahut, Louise-Anne Fillot, Didier R.*

*Long, Paul Sotta*

